Reversible Structural Swell−Shrink and Recoverable Optical Properties in Hybrid Inorganic−Organic Perovskite

Yupeng Zhang,[†,⊥] Yusheng Wang,[‡,⊥] Zai-Quan Xu,[†,⊥] Jingying Liu,[†] Jingchao Song,[†] Yunzhou Xue,[†,‡] Ziyu Wang,[†] Jialu Zheng,[†] Liangcong Jiang,[†] Changxi Zheng,[§] Fuzhi Huang,[†] Baoquan Sun,[‡] Yi-Bing Cheng,[†] and Qiaoliang Bao[*,‡,†]

[†]Department of Materials Science and Engineering, Monash University, Wellington Road, Clayton, Victoria 3800, Australia

[‡]Institute of Functional Nano and Soft Materials (FUNSOM), Jiangsu Key Laboratory for Carbon-Based Functional Materials and Devices, and Collaborative Innovation Center of Suzhou Nano Science and Technology, Soochow University, Suzhou 215123, People's Republic of China

[§]Department of Civil Engineering, Monash University, Clayton 3800, Victoria, Australia

[⊥]These authors contributed equally to this work.

*Email: qlbao@suda.edu.cn (Q. Bao)

Figure 1 g–i showed the morphologies of perovskite films with different MA/Pb ratios. From these images it is very clear that the increase of MA^+ content results in the formation of perovskite films with small grain size. In general, a solution precipitation process involves two steps: nucleation and crystal growth. Nuclei will form when a solution reaches supersaturation and the volume of the nuclei in the system would depend on the rate of nucleation and the degree of the supersaturation. The increase of MA^+ content results in a high degree of supersaturation, which favors the crystal growth of a large number of nuclei, thereby promoting the formation of perovskite films with small grain size.

The hybrid organic-inorganic perovskite microwires were prepared by a two-step method, as schematically shown in Figure S1a. The high quality PbI_2 microwires were firstly synthesized using a solution process. In general the solvent medium and temperature in solution process are key factors that affect the crystallinity, morphology and texture of the precipitated crystals. Owing to the different solubility of PbI_2 in DMF and water, we developed a crystallization method to prepare PbI_2 microwires. By controlling the DMF/water ratio and inversing the growth temperature, the resulting PbI_2 microwires with different diameters and lengths could be produced. The optical and low magnification TEM images of PbI_2 microwire are shown in Figure S1b and 1c, revealing smooth surface and highly crystalline structure with a length up to 80 μm. The corresponding selected area electron diffraction (SAED) pattern shown in inset of Figure S1c confirms the single crystalline character of the PbI_2 microwire. The $MAPbI_3$ perovskite microwires were then formed through intercalating the MAI molecules into the interval sites of PbI_6 octahedrons layers. The $MAPbI_3$ perovskites still maintains the wire shape as displayed in Figure S1d, indicating the good morphology retention after vapour phase conversion. The slight difference in optical contrast between the perovskite and PbI_2 microwires could be attributed

to the different light absorbance in these two materials as well as different light reflection from wire surface.

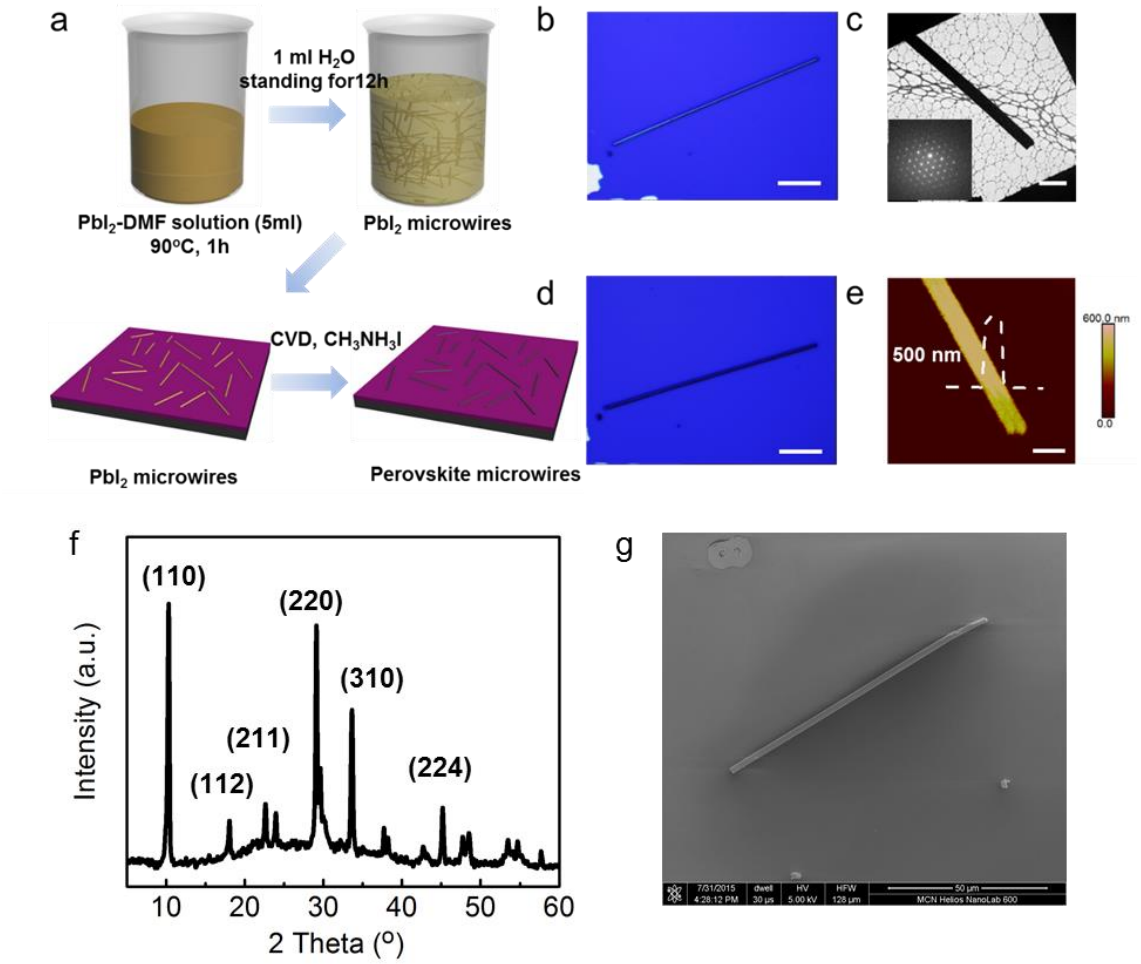

Figure S1. (a) Schematic illustration for solution process to fabricate PbI_2 microwires and vapour phase conversion process from PbI_2 to $CH_3NH_3PbI_3$ microwires. (b) Optical image of PbI_2 microwires. Scale bar, 20 μm. (c) TEM images of a typical PbI_2 microwire and its corresponding SAED pattern. Scale bar, 1 μm. (d) Optical image of a perovskite microwire. Scale bar, 20 μm. (e) AFM height image of a perovskite microwire. Scale bar, 1 μm. (f) XRD pattern of perovskite microwires. (g) SEM image of single perovskite microwire.

In order to prevent contamination from doping perovskite, a lithography-free technique based on evaporation through hard Si_3N_4 shadow mask was used to fabricate high quality and clean single wire device, as shown in Figure S2. First, perovskite microwires were grown on a SiO_2 (thickness: ~300 nm)/p-Si substrate. Second, a Si3N4 shadow mask designed and

milled using a focused ion beam (FEI Helios, Dual Beam) was used to define the electrodes. Third, the sample and the mask were aligned using a customized X-Y-Z micropoitioner before Ti/Au (5nm/100nm) were deposited suing an electron beam evaporator.

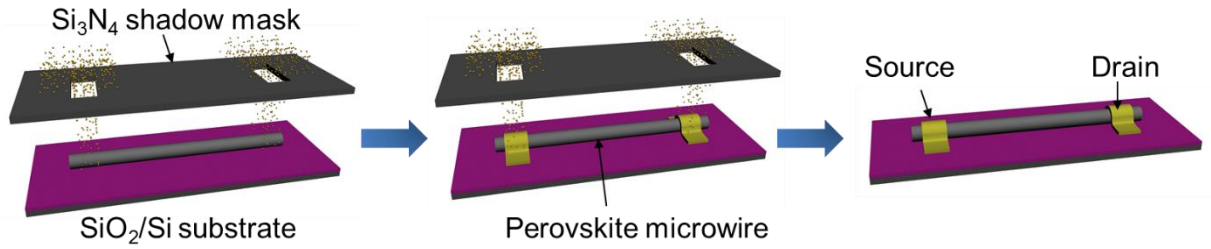

Figure S2. Schematic illustration for fabrication of perovskite single wire device by using a lithography-free technique based on evaporation through hard Si_3N_4 shadow mask.

Table 1. The lattice constants of tetragonal perovskite (A_yBX_3) with different filling of MA^+

y	Lattice type	Lattice constants, *a*, *b* and *c* in Å
0	monoclinic	*a*=9.2636, *b*=9.3043, *c*=11.7845, *α*=90.00°, *β*=90.00°, *γ*=100.48°
0.25		*a*=8.6613, *b*=8.9722, *c*=12.1651, *α*=90.00°, *β*=90.00°, *γ*=86.43°
0.5		*a*=9.2047, *b*=8.9159, *c*=12.3357, *α*=90.00°, *β*=90.00°, *γ*=86.53°
0.75		*a*=8.9251, *b*=8.9608, *c*=12.6323, *α*=90.02°, *β*=90.29°, *γ*=89.35°
1	Tetragonal	*a*=*b*=9.2419, c=12.8838, α=β=γ=90.00°

According to the DFT simulation, we can find the change of lattice constants with different MA^+ contents in perovskites. In particular, the lattice changes from monoclinic to tetragonal with a change in *a*. This means that increasing the content of MA^+ causes shear stress in *b*-*c* plane. Moreover, increasing the content of MA^+ stretches the cell in *c* direction. This combined lattice changes will be translated into volume expansion

Table 2. The lattice constants of cubic perovskite (A_yBX_3) with different filling of MA^+

y	Lattice type	Lattice constants, *a*, *b* and *c* in Å
0	monoclinic	*a*=5.9298, *b*=5.9005, *c*=7.3868, *α*=93.76°, *β*=90.00°, *γ*=90.00°
0.125		*a*=6.1210, *b*=4.7879, *c*=8.2370, *α*=94.15°, *β*=90.00°, *γ*=89.72°
0.25		*a*=6.0212, *b*=6.0758, *c*=6.8607, *α*=90.67°, *β*=90.00°, *γ*=90.00°
0.375		*a*=6.0888, *b*=6.2178, *c*=6.5732, *α*=89.91°, *β*=90.00°, *γ*=90.00°
0.5		*a*=6.2818, *b*=6.3236, *c*=6.4012, *α*=90.03°, *β*=90.00°, *γ*=90.00°
0.625		*a*=6.3490, *b*=6.3815, *c*=6.3660, *α*=90.65°, *β*=90.00°, *γ*=90.00°
0.75		*a*=6.3848, *b*=6.4200, *c*=6.3802, *α*=90.59°, *β*=90.00°, *γ*=90.00°
0.875	monoclinic	*a*=6.3863, *b*=6.3756, *c*=6.3547, *α*=91.15°, *β*=90.00°, *γ*=90.00°
1	Cubic	*a*=*b*=*c*=6.4918, *α*=*β*=*γ*=90.00°

These results show that similar to tetragonal A_yBX_3, the increase of MA^+ transforms the lattice from monoclinic to cubic. The length of the c-axis is increased and shear stress in the *a*-*b* plane is introduced, which consequently changes the *γ*-angle.